

Initiation and propagation of a crack in the orthopedic cement of a THR using XFEM

Bachir Gasmi^{1,2}, Sahli Abderrahmene^{1,2}, Benbarek Smail*¹ and Aour Benaoumeur^{1,2}

¹Laboratory of Physics and Mechanical Materials (LMPM), University Djillali Liabes of Sidi Belabbes, BP89 Cite Larbi ben Mhidi, 22000n Algeria

²Department of Mechanical Engineering, National Polytechnic School of Oran, BP1523 El Mnaour 31000, Oran, Algeria

(Received January 25, 2019, Revised May 30, 2019, Accepted June 15, 2019)

Abstract. The sealing cement of total hip arthroplasty is the most widely used binder in orthopedic surgery for anchoring implants to their recipient bones. Nevertheless, this latter remains a fragile material with weak mechanical properties. Inside this material cracks initiate from cavities. These cracks propagate under the effect of fatigue and lead to the failure of this binder and consequently the loosening of the prosthesis. In this context, this work consists to predict the position of cracks initiation and their propagations path using the Extended Finite Element Method (XFEM). The results show that cracks can only be initiated from a sharp edges of an ellipsoidal cavity which the ratio of the minor axis over the major axis is equal to 0.1. A maximum crack length of 19 μm found for a cavity situated in the proximal zone position under a static loading. All cracks propagate in same(almost) way regardless of the cavity(site of initiation) position and its inclination in the proximal zone.

Keywords: total hip replacement; XFEM; orthopedic cement; cavity; damage; crack propagation

1. Introduction

The mechanical strength of the total hip replacement (THR) depends essentially on the used cement nature. The main role of this latter is to ensure a good implant-bone adhesion and to homogenize the load transfer between the implant and the bone Pauwels (1973). Because of its fragile nature and its low mechanical properties, the cement is the weakest link in the implant-cement-bone load transfer chain. It breaks the first by presenting voids or microcracks at the cement, which over time become larger under fatigue load causing the failure of the cement and consequently the loosening of the implant inside the bone (Maloney *et al.* 1989, K.A. Mann 2004).

Under the effect of the mechanical stresses, the cement must be able to withstand the initiation and propagation of cracks which can lead to its damage and consequently to its loosening as shown by Jasty *et al.* (1991), K.A. Mann (2004) and Sahli A. (2014) investigate the stress field in the cement in order to know the zones subjected to high stresses and consequently predict zones that can be subjected to cracks initiation .Murphy BP(2002) and Lennon(2003) researches of implants subjected to bending and torsion loads show that a gradual process of damage can occur by a form of initiation and accumulation of mechanical failure of severals microcracks initiated

*Corresponding author, Professor, E-mail: sma_benbarek@yahoo.fr

from pores within the bulk cement mantle.

Several numerical studies have modeled the orthopedic cement damage such as Topoleski (1993) and Mann K.A. (2000). The majority of these works has focused on particular modes of damage, such as the propagation of cracks (Benouis Ali 2015), fracture (N. Bounoua 2014), fatigue (Fritsch E. 1996), and the debonding (M. A. Perez 2010).

The use of the eXtended Finite Element Method (XFEM) is recently used as a reliable way to investigate the crack propagation parameters as stress intensity factors (SIF) and crack path. Among these works one can cite the work of Majid Jamal Omid (2014), S. Shojaee (2013) and A. Benzaama (2018). Therefore, this technique can be used to investigate the fracture behavior of the orthopedic cement of the total hip arthroplasty.

Knowledge of areas experiencing a high degree of damage as well as the estimation of the length of crack in the cement likely to expose the risk of rupture of the implanted prosthesis in patients is very important and the ways to stop them as shown by Bouiadjra B. (2014).

The objective of this work is to study the effect of the presence of different shapes and positions of micro-cavities on the of crack initiation risk and its site in the orthopedic cement using the Extended Finite Element Method (XFEM). This study predicts also very well the cracks propagations paths for all initiated cracks.

2. Modeling of Crack initiation

2.1 The cohesive zone concept

The concept of the cohesive zone was introduced by Dugdale, D.S. (1960) and Barenblatt, G. (1962) in the 1960s. With the improvement of numerical modeling tools, this concept has become a model of crack propagation widely used in finite element analysis because of its simplicity and its multiple use possibilities.

2.1.1 Principle of cohesive zone models

The cohesive zone models describe the area at the crack tip where the material is damaged using a relation between the cohesive stress vector (cohesive forces per unit area) and the jump of displacement between the crack lips opening (vector of the crack opening). The use of this model is accomplished by employing cohesive elements, whose behavior is governed by the traction-separation law, which reflects the progressive degradation of the material during the loading. The cohesive elements make possible to represent the reduction of the cohesive stresses during the progressive damage of the material.

2.1.2 Crack initiation criteria

In the considered finite element model, a criterion controls the beginning of damage of the cohesive element, while its evolution is controlled by a propagation criterion (Krishna Siva 2011, ABAQUS documentation 2011). Damage initiation takes place when stresses or deformations satisfy the damage beginning criterion. For example, Abaqus software considers six criteria, which involve the maximum components of the stress vector and the corresponding maximum strains (Wolff 1992). When the maximum principal stress or the maximum principal strain criterion is met, a new crack is initiated. This crack is always orthogonal to the direction of the maximum principal stress.

- The maximum principal stress criterion

In this study, the criterion of maximum principal stress is chosen. This criterion can be represented as follows (ABAQUS documentation 2011):

$$f = \left\langle \frac{\sigma_{max}}{\sigma_{max}^0} \right\rangle \quad (1)$$

Here, σ_{max}^0 represents the maximum allowable principal stress. The symbol $\langle \rangle$ represents the Macaulay bracket with the usual interpretation (i.e., $\langle \sigma_{max} \rangle = 0$ if $\langle \sigma_{max} \rangle < 0$ and $\langle \sigma_{max} \rangle = \sigma_{max}$ if $\sigma_{max} \geq 0$).

The Macaulay brackets are used to signify that a purely compressive stress state does not initiate damage. This latter is assumed to initiate when the maximum principal stress ratio (as defined in the expression above) reaches a value of one.

- **Damage evolution criterion**

When the priming criterion is reached, the progressive damage of the cohesive elements is described by the damage variable D , the value of which changes from 0 to 1. The cohesive stresses T_n and T_t are then calculated by the following expressions (Sahli 2014):

$$T_n = \begin{cases} (1 - D)\bar{T}_n & \text{if } \bar{T}_n \geq 0 \\ 0 & \text{if } \bar{T}_n < 0 \end{cases} \quad (2)$$

$$T_t = (1 - D)\bar{T}_t \quad (3)$$

Where \bar{T}_n and \bar{T}_t are the normal and shear stress components predicted by the elastic traction-separation behavior for the current separations without damage. To describe the evolution of damage under a combination of normal and shear separations across the interface, we introduce an effective opening δ_m , defined as follows:

$$\delta_m = \sqrt{\langle \delta_n^2 \rangle + \delta_t^2} \quad (4)$$

Only two types of evolution law of variable D are widely used: linear (Figure 1.a) or nonlinear (Figure 1.b). The proposed model is based on the work of Turon *et al.*

3. Geometry and finite element model

Figure 2 shows a longitudinal cross section of the THP model. The thickness of the orthopedic cement has been taken equal to 2 mm to ensure an even transfer of the load to the bone.

3.1 Materials

The mechanical properties of the total hip replacement's elements are shown in Table 1. In this study, all the components of the numerical model were considered as elastic linear materials.

3.2 Boundary conditions

The value of the force acting on the head of the femur has been taken according to the study conducted by Burstein A.H. (2009). He found that this force is four times the weight

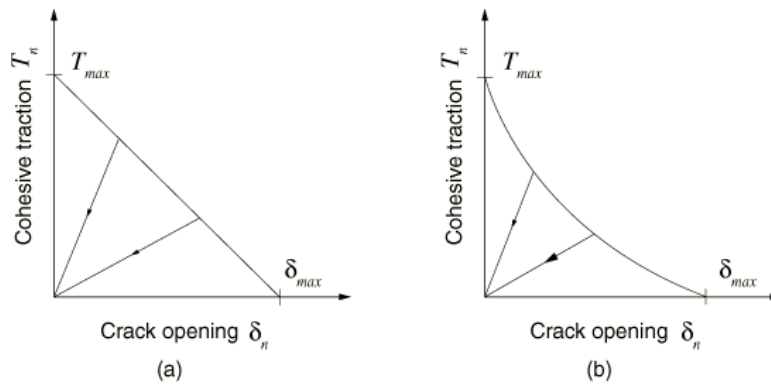


Fig. 1 Typical linear (a) and nonlinear (b) traction-separation response.

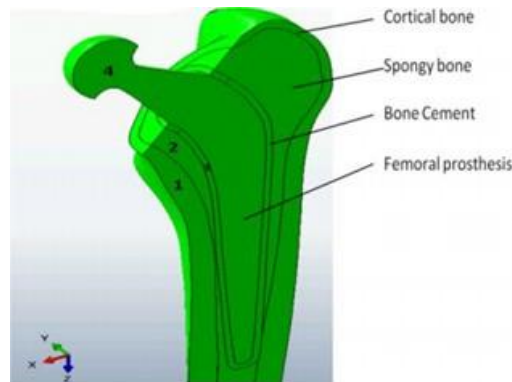


Fig. 2 Longitudinal section of the THP model.

Table 1 Mechanical properties of THR components (Bouziane 2010, Burstein 1973, Burstein 2009)

Cortical bone	17000	0.3
Spongy bone	2000	0.3
Cement (PMMA)	2300	0.3
Implant	210000	0.3

3.3 Boundary conditions

The value of the force acting on the head of the femur has been taken according to the study conducted by Pustoch *et al.* (2009). Indeed, this latter is four times the weight of the human body. A value of 2.5 KN exerted on the femur head is considered for the finite element analysis. The distal epiphysis is considered fully embedded. Figure 3 shows the boundary and loading conditions applied on the THR.

3.4 Mesh of the global model

The reliability of the obtained results requires a very refined mesh. Indeed, cement is a determining element of the prosthesis. The refinement of its mesh is of great importance for the



Fig. 3 Boundary and loading conditions applied on THR

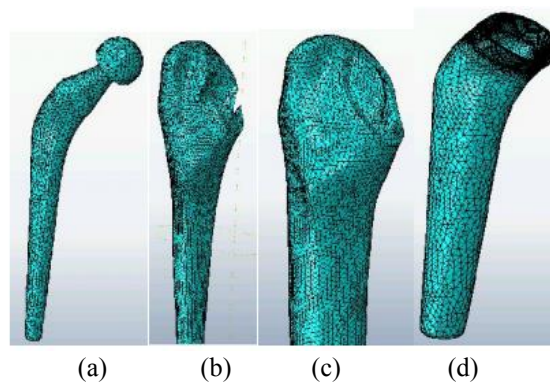


Fig. 4 Mesh of all THR components: (a) implant, (b) sponge bone, (c) cortical bone and (d) cement

analysis of the structure. Figure 4 illustrates the meshing of different THR components. It also shows a refinement of the stress concentration zone mesh studied.

3.5 Positions of the studied defects

Cement is a very decisive element of the total hip replacement. Its analysis is of great importance for the lifespan of this latter. By analyzing the stress distribution in the cement (Fig. 5), it can be seen that there are two zones of high Von Mises stress concentration. They are located in the top regions where the cement is in direct contact with the cortical bone. In the rest of this structure, the stresses remain very low.

In this study, the sub-model technique is used to facilitate the cavity shape changes and its position (Fig. 6). For each position, the angle of the cavity inclination is varied around an axis of

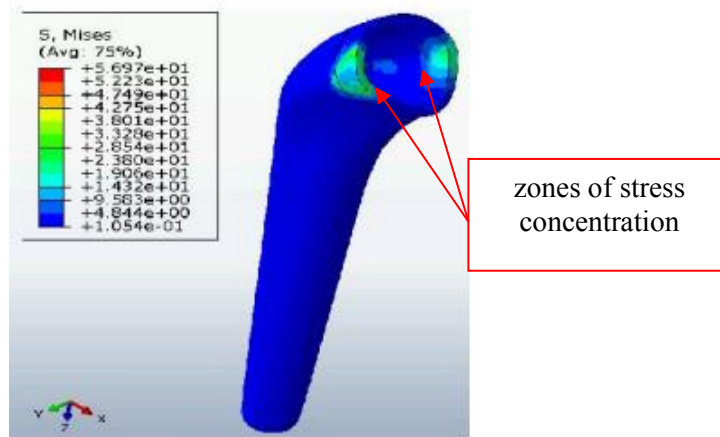


Fig. 5 Distribution of Von Mises stresses in orthopedic cement.

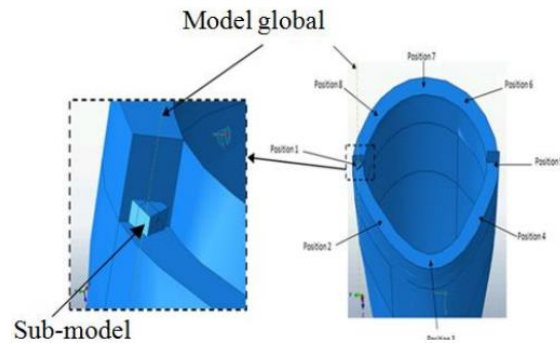


Fig. 6 Illustration of the submodel technique and the different positions of the defects (cavities)

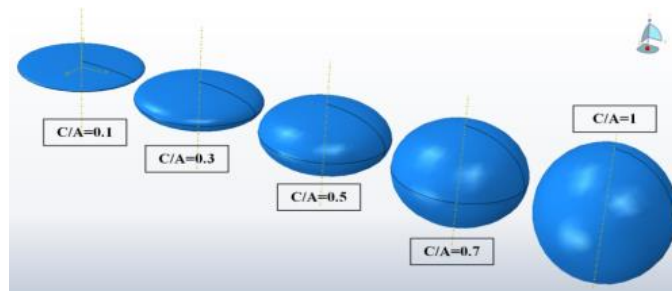


Fig. 7 The different cavity shapes studied by numerical simulation

rotation perpendicular to sagittal plane with a step of 15 degrees with for different cavity shapes. It should be noted that the zones of high stress concentration are located in positions 1 and 5 as shown in figure 6.

3.6 Cavity shapes

In order to study the damage caused by the presence of cavity in the orthopedic cement, five different shapes have been selected. If C is the little diameter and A the greater one, the different

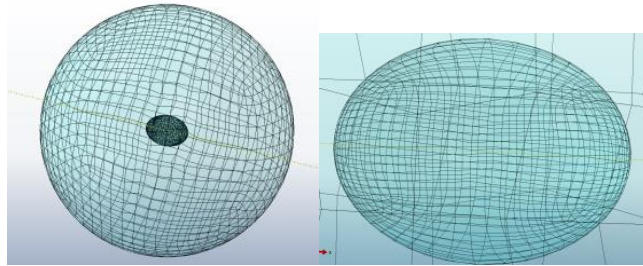


Fig. 8 Schematic representation of the submodel mesh

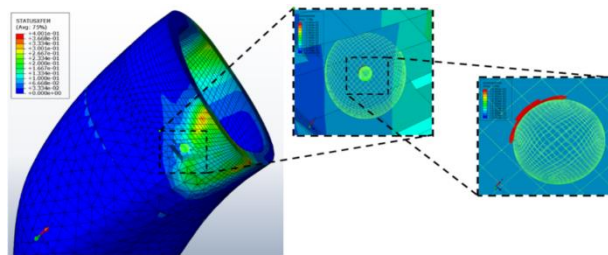


Fig. 9 Sub-model results within the global model

ratios are $C/A = \{0.1, 0.3, 0.5, 0.7 \text{ and } 1\}$ (Fig. 7). The attention is made on the both dangerous positions (1 and 5) by also varying the cavity orientation.

A very refined mesh of the subdomain including the cavity has been used in order to obtain a good evaluation of the damage. Figure 8 shows the mesh used for the sub-model. Noting that the mesh of the global model is kept the same used for the previous calculation (without cavity).

4. Results and discussion

4.1 Illustration of damage

The numerical simulation was carried out using the submodel technique. Figure 9 shows a crack initiation (prediction) from a cavity with a shape of $C/A = 0.1$ oriented with 90° relative to the sagittal plane in the position 1 of the proximal zone. This figure clearly shows the initiation (first elements row) and the propagation (second elements row) of a crack emanating from the cavity under the considered static loading. Those figure shows clearly the reliability of the used criterion by predicting the crack initiation and propagation at the right place (the sharp edge of the cavity).

In Figures 10.a-b and 10.c-d is presented a crack initiation and propagation from an ellipsoidal cavity with a ratio $C/A = 0.1$ for both positions 1 and 5 respectively. This results show the efficiency of the use of XFEM for the quantification of the damage mechanisms (crack initiation) which can take place during the initial stages of cracking (typically when the crack is localized in ten micrometers). The analysis of the obtained results shows that the crack propagation is localized on a well-defined planes which probably correspond to the most stressed ones. Access to the 3D morphology of the crack shows that the crack front is continuous in space and correspond to the plane of the maximum principal stress.

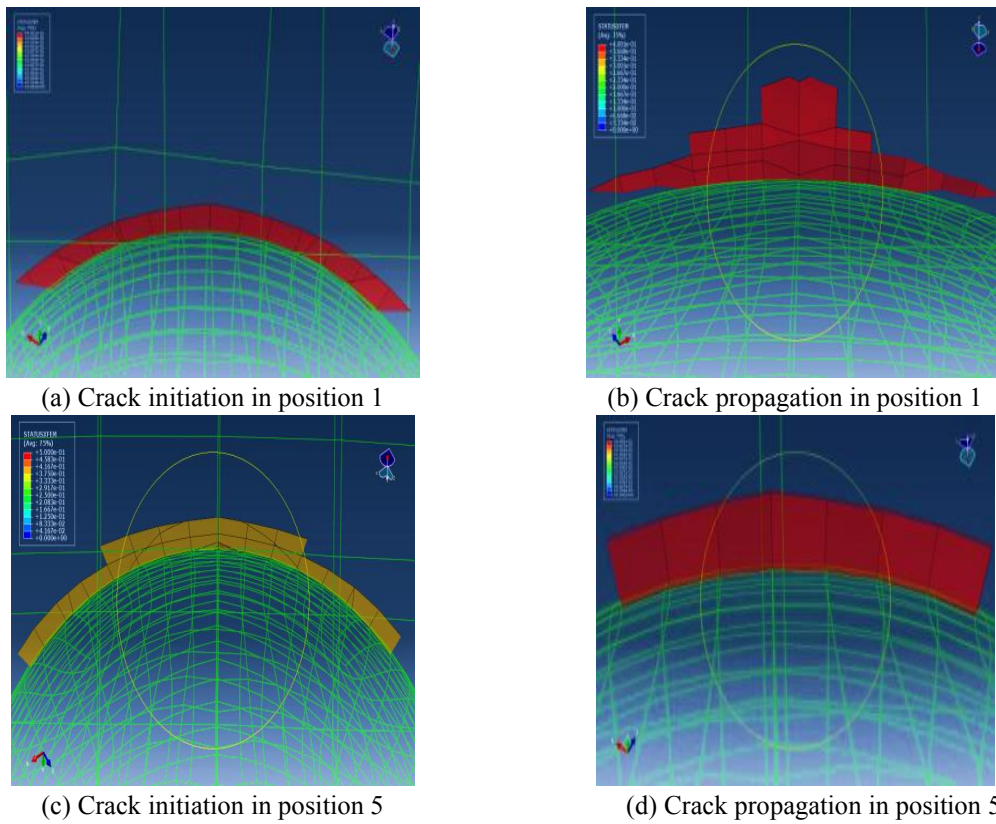


Fig. 10 Illustration of cracks initiation and propagation for both positions: (a-b) position 1 and (c-d) position 5

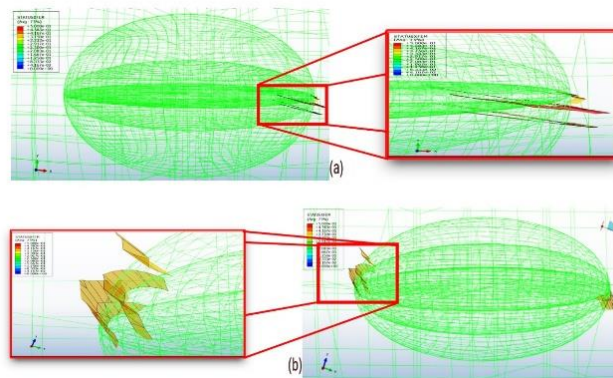


Fig. 11 Illustration of cracks for different cavity shapes in the distal area: (a) Position 1, (b) Position 5

4.2 Effect of the cavity shape on the damage of the orthopedic cement

In this section, an emphasis is taken on the effect of the cavity shape on the orthopedic cement's damage. Figures 11.a and 11.b illustrate the superposition of three types of cavity (C/A =

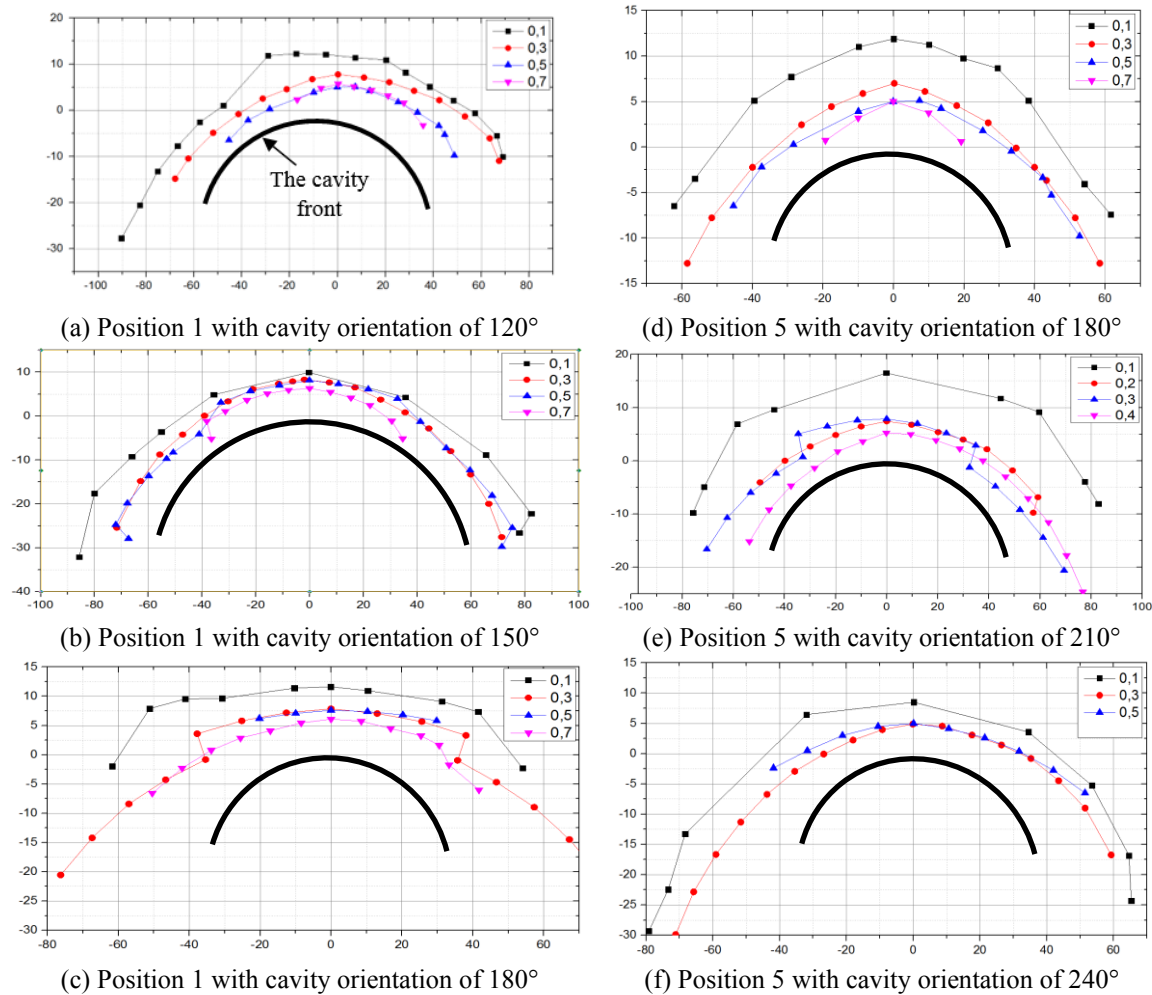


Fig. 12 Evolution of the crack front for different cavity shapes for positions 1 and 5 of the distal zone

0.1, 0.3, 0.5) for positions 1 and 5 respectively. It can be noticed that the cavity shape has no influence on the crack orientation but on the other hand it influences the crack initiation position. It is also noted that the shape of the cavity has a significant effect on the crack size.

To measure the crack size, the crack front is plotted on a coordinate system for different cavity shapes and orientations. All the observed fronts are plotted on the same graph as illustrated in Figure 12. From these illustrations, it can be seen that the crack length is proportional to the cavity shape, the more the cavity is flat the more the crack is bigger. This result seems logical if we consider that crack's size is directly related to the value of the tensile stress. However, it may be noted that the crack sizes tend to equal as the cavity tend to get the spherical shape. These results also show that position 5 gives bigger crack than the position 1.

4.2 Effect of the cavity orientation on the damage of the orthopedic cement

In Figures 13.a and 13.b, we presented respectively a superposition of crack initiation from several cavity inclinations for positions 1 and 5. In the case the cavity shape corresponds to $C/A =$

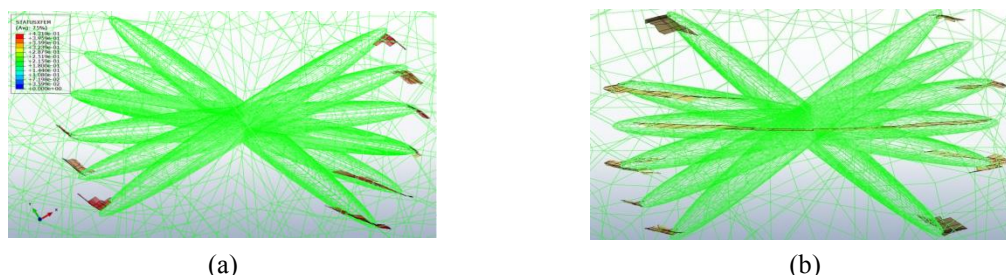


Fig. 13 Illustration of the crack initiation for different cavity inclinations, (a) Position 1, (b) Position 5

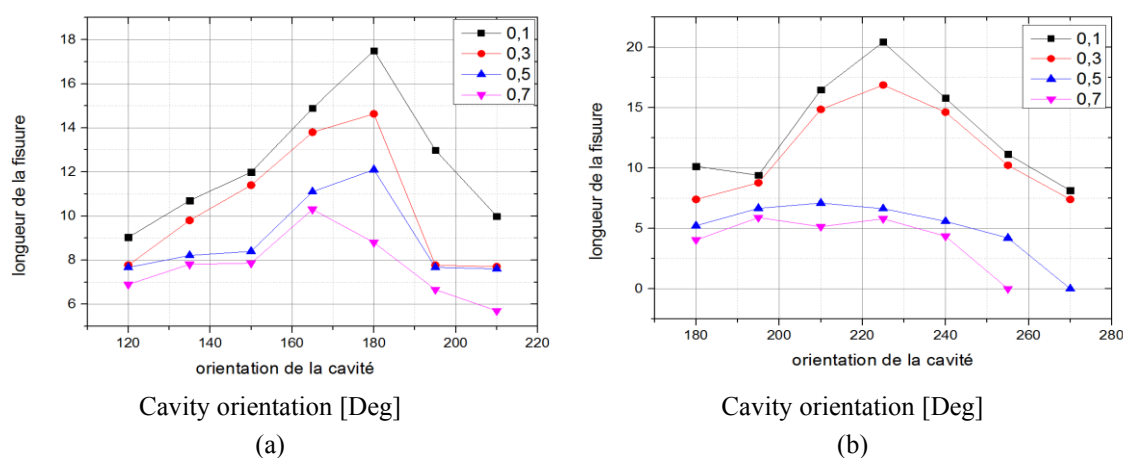


Fig. 14 Evolution of the maximum crack length for different cavity shapes and inclinations in both cases: (a) Position 1 and (b) Position

0.1. By observing the three-dimensional crack initiation and propagation, it can be noted that the crack propagation occurs in one plane for different cavity orientations(any where the crack is initiated, it will propagate in one direction). Indeed, the cavity inclination influences the crack length: The more the cavity inclination the more is the crack size.

In order to highlight the influence of the cavity shape on the crack length, we measured the maximum crack length for each orientation and we plotted the evolution of this latter for different cavity shapes in the positions 1 (Fig. 14.a) and position 5 (Fig. 14.b). It can be seen that the crack length increases with respect to the crack orientation until a reaching a maximum and then it decreases. Moreover, the influence of the cavity shape is significant for the cavity shape ratio $C/A = 0.1$, it decreases when C/A increase. A maximum crack length about $19\mu\text{m}$ is recorded for a cavity located at position (5) in the proximal zone corresponding to 225° cavity inclination.

5. Conclusions

If the presence of cavities in the orthopedic cement sealing the total hip prosthesis is inescapable, it has the inconvenience of being the site of the stress concentration causing crack initiation which leads to the loosening of the prosthesis. This study was carried out with the aim of analyzing the crack initiation and propagation from a localized cavity with various shapes in the

cement fixing the hip prosthesis by using the extended finite element method. According to the obtained results, it is possible to draw the following conclusions:

- Using the XFEM method, the path of a crack initiated from a cavity in the cement of the THR can be predicted and then the lifespan of the THR can be predicted to.
- The most significant damage in the cement is located at the sharp edge of the ellipsoidal cavity when the ratio $C/A = 0.1$, i.e. a flat cavity.
- The maximum crack length ($19 \mu\text{m}$) is recorded for a cavity located in position (5) of the proximal zone with an inclination equivalent to 225° .
- The crack orientation adopts the same plane of propagation for all cavity orientations because the crack is too small to disturb the surrounding stresses field.
- The obtained results also show that the cracks lengths obtained in position 5 are greater than that noted in position 1.

References

- Pauwels, F. (1973), *Atlas zur Biomechanik der gesunden und kranken Huft*, Springer Verlag, Berlin, Germany.
- Jasty, M., Maloney, W.J., Bragdon, C.R., O'Connor, D.O., Haire, T. and Harris, H.H. (1991), "The initiation of failure in cemented femoral components of hip arthroplasties", *J. Bone. Joint Surg. Br.*, **73B**(4), 551-558. <https://doi.org/10.1302/0301-620X.73B4.2071634>.
- Maloney, W.J., Murali, J., Burke, D.W., O'Connor, D.O., Zalenski, C. and Braydon, E.B. (1989), "Biomechanical and histologic investigation of cemented total hip arthroplasties", *Clin. Orthop. Rel. Res.*, **249**, 129-140.
- Mann, K.A., Gupta, S., Race, A., Miller, M.A., Cleary, R.J. and Ayers, D.C. (2004), "Cement microcracks in thin-mantle regions after in vitro fatigue loading", *J. Arthroplasty*, **19**, 605-612. <https://doi.org/10.1016/j.arth.2003.12.080>.
- Sahli, A., Benbarek, S., Bouiadjra, B. and Bouziane, M. (2004), "Effects of interaction between two cavities on the bone cement damage of the total hip prosthesis", *Mech. Mech. Eng.*, **18**(2), 107-120.
- Bouiadjra, B., Belarbi, B., Benbarek, S., Achour, T. and Serier, B. (2007), "Finite element analysis of the behaviour of crack emanating from microvoid in cement of reconstructed acetabulum", *Comput. Mater. Sci.*, **45**(1-2), 385-391. <https://doi.org/10.1016/j.msea.2006.12.087>.
- Dugdale, D.S. (1960), "Yielding of steel sheets containing slits", *J. Mech. Phys. Solids*, **8**(2), 100-104. [https://doi.org/10.1016/0022-5096\(60\)90013-2](https://doi.org/10.1016/0022-5096(60)90013-2).
- Barenblatt, G. (1962), "The mathematical theory of equilibrium cracks in brittle fracture", *Adv. Appl. Mech.*, **7**, 55-129. [https://doi.org/10.1016/S0065-2156\(08\)70121-2](https://doi.org/10.1016/S0065-2156(08)70121-2).
- Rudraraju, K.S.S. (2011), "On the theory and numerical simulation of cohesive crack propagation with application to fiber-reinforced composites", Ph.D. Dissertation, University of Michigan, 2011.
- ABAQUS, A.V. (2011), *6.11 Documentation*, ABAQUS Inc., Sunnyvale, CA, USA.
- Wolff, J. (1992), *Das Gezetz der Transformation des Knochens*, Hirschwald, Berlin, Germany.
- Bouziane, M.M. (2010), "Finite element analysis of the behavior of microvoids in the cement mantle of cemented hip stem: Static and dynamic analysis", *Mater. Design*, **31**(1), 545-550. <https://doi.org/10.1016/j.matdes.2009.07.016>.
- Burstein, A.H., Reilly, D.T. and Frankel, V.H. (1973), "Failure characteristics of bone and bone tissue", *Perspectives in Biomedical Engineering*, The MacMillan press, London, 131-134.
- Pustoch, A. and Cheze, L. (2009), "Normal and osteoarthritic hip joint mechanical behavior: A comparison study", *Med. Biol. Eng. Comput.*, **47**, 375-383. <https://doi.org/10.1007/s11517-009-0457-9>.